Optimum Design of Ceramic Spray Coating Evaluated in Terms of Intensity of Singular Stress Field

Zefeng Wang, Nao-Aki Noda*, Masayasu Ueno and Yoshikazu Sano

Department of Mechanical Engineering, Kyushu Institute of Technology,

1-1 Sensui- cho, Tobata-ku, Kitakyushu-shi, Fukuoka, 804-8550 Japan

E-mail: noda@mech.kyutech.ac.jp

Hearth rolls are the most important tools in continuous annealing line to produce thin steel sheet. Usually the roll surface is coated by ceramics using thermal spraying. However, material mismatch and temperature change may cause thermal stress leading to the failure of the coating and deteriorating high adhesive strength and wears resistance. Therefore, it is very important to improve the debonding strength by optimizing the design of spray coating. The traditional method of evaluating the debonding strength of spray coating is prescribed as JIS H8304 thermal test. This paper focuses on the intensity of singular stress field (ISSF) at the end of interface since few research is available in terms of ISSF. Previously the authors considered the JIS specimen assuming a plane strain. However, since the hearth roll is cylindrical and axi-symmetric, the difference between plane strain and axi-symmetric models should be clarified. Thus in this paper the axi-symmetric model is newly considered and the optimum design is discussed by varying the coating material and the coating thickness. Also the present results are compared with the previous results of JIS specimen so that the difference between actual model and JIS specimen can be clarified to contribute the design and evaluation of the real rolls.

1. Introduction

Continuous annealing furnace is the common line to produce steel sheet used in automobiles. Here, the rolls are working in a harsh environment whose temperature is usually between 700℃ and 800℃ and sometimes up to 1200℃ for some special grade requirement. [1] Therefore, excellent performances are demanded for roll material and structure. First of all, the roller surface should be able to do against corrosion and oxidation at high temperatures. Secondly, it must be wear-resistant with a longer service life. [7] For this demand, the ceramic spaying coating as shown in **Figure 1(a, b)** has been widely used in recent decades. [2,3] To prevent the coating failure due to material mismatch under cyclic thermal shock, the multi-layer coating as shown in **Figure 1(b)** is usually employed instead of single splay coating.

In order to improve the coating strength and service life, different processes and several materials have been widely studied as well as the debonding strength evaluation method. In Japan, the thermal shock resistance of the spaying coating structure is prescribed as JIS8304 (2007) with the specimen shown in **Figure 1(c)**. [4] Mutoh et al have reported the thermal shock damage characteristics based on the experiment and finite element analysis. [5] To evaluate the interfacial strength of dissimilar adhesive structures more accurately, it is desirable to consider the intensity of singular stress field (ISSF) at the interface end. Since few studies are available for ISSF on this multi-layer structure under thermal shock, Noda, et al proposed a convenience evaluation method for spray coating in terms of on ISSF. [6] The previous study considered the JIS specimen assuming two-dimensional plane strain, while the hearth roll is cylindrical and axi-symmetric as shown in **Figure 1(e)**. Since the difference between these two models cannot be ignored especially for small roller diameters, in this paper the axi-symmetric model will be considered and the optimum design will be discussed by varying the coating material and the coating thickness. Then, the results will be compared

with the previous 2D results for JIS specimen so that the difference between actual axi-symmetric shape and JIS specimen can be clarified.

2. Nomenclature

In this paper the following notations are used.

12YZ	Coating material which contains 12% Y_2O_3
20YZ	Coating material which contains 20% Y_2O_3
8YZ	Coating material which contains 8% Y_2O_3
C	Specific heat
E	Young's modulus
E_1	Young's modulus of the top coating
E_2	Young's modulus of the bonded coating
E_3	Young's modulus of the substrate
G	Shear modulus
G_1	Shear modulus of the top coating
G_2	Shear modulus of the bonded coating
G_3	Shear modulus of the substrate
H	Thickness of the top coating
ISSF	Intensity of singular stress field
K	Thermal conductivity
K_σ	Intensity of singular stress field (ISSF)
K_σ^{Axial}	ISSF of axi-symmetric model
R	Distance from the end of the interface

R_{inf}	Inner radius R in the Fig 6(a) when R is large enough
W	Width of the substrate layer
e_{min}	The minimum element size in simulation
h	Thickness of the bonded coating
ℓ	Thickness of the substrate layer
r	The radial distance in the polar coordinates
u_{r0}^{AXIAL}	Displacement in the axial direction
α , β	Dundurs' parameters
α_1	Dundurs' parameter of the top coating
α_2	Dundurs' parameter of the bonded coating
α_e	Coefficient of expansion
ϒ	Poisson's ratio
Υ_1	Poisson's ratio of the top coating
Υ_2	Poisson's ratio of the bonded coating
Υ_3	Poisson's ratio of the substrate
λ	Singular index defined in
κ_j	$$\kappa_j = \begin{cases} \dfrac{3-\nu_j}{1+\nu_j}\left(plane\ stress\right) \\ 3-4\nu_j\left(plane\ strain\right) \end{cases} \left(j=1,2\right)$$ Kolosov constant defined by equation2
κ_1	Kolosov constant of the top coating
κ_2	Kolosov constant of the bonded coating
σ_y	Stress in the y direction in Fig 1 (d)
σ_0	Non-singular term defined by equation 5
$\tilde{\sigma}_r$	Non-singular term in the radial direction

4

$$\sigma_r^{Axial}$$ Stress in the axial direction

$$\Delta\alpha$$ $$\Delta\alpha = \begin{cases} \alpha_1 - \alpha_2 & \text{(plane stress)} \\ (1+\nu_1)\alpha_1 - (1+\nu_2)\alpha_2 & \text{(plane strain)} \end{cases}$$

$$\Delta E$$ $$\Delta E = \dfrac{8}{\left\{ \dfrac{(\kappa_1 - 3)}{G_1} - \dfrac{(\kappa_2 - 3)}{G_2} \right\}}$$

$$\Delta T$$ Temperature change of the specimen

3. Material properties and analysis model

The process of thermal shock test specified by JIS8304 (2007) is shown in **Figure 2(a)**. First the specimen is heated up to 1000℃ and keep the temperature for a 1800s to ensure uniform heating of the specimen, then the specimen is merged into water of 20℃ to simulate the rapid cooling. That cycle repeats again and again until the failure of coating occurs. In this test the failure usually occur at the interface end of bond coating and top coating.

The JIS specimen is a cubic SU304 steel coated with yttrium (Y_2O_3) stabilized zirconia (ZrO_2). The top coating ZrO_2 has 8wt% ~ 20wt% of Y_2O_3 (In the following % will be omitted) and the substrate are bonded with CoNiCrAlY. The material properties are shown in **Table 1**. **Figure 3** shows the material properties of three layers: coefficient of expansion α_e, specific heat C, Young's modulus E and thermal conductivity K. All material properties are temperature dependent.

Different from the previous study asuming plane strain as shown in **Figure 1(d)** of the JIS specimen, here the axi-symmetric model shown in **Figure 1 (f)** is used as the analysis model so that the results of actual structure and experimental specimen can be compared. Here the subscript 1, 2, 3 represents the top coating, bond coating and substrate respectively, with the corresponding material properties shown in **Table 1**. Our previous studies show that the

ISSFs of bonded cylinder as well as pipe are quite different from the ISSF of bonded plate by up to 30%[12, 13]. Therefore the different between the problem in **Figure 1 (d)** and **Figure 1 (f)** will be clearified in this study.

In the analysis of this research, FEM is use to obtain the value of stress at the end of interface when simulating the thermal shock. In this study, FEM software ANSYS 16.2 with 4 nodes quad element is applied to thermal-structural elastic analysis.

4. Axi-symmetric analysis method for the intensity of singular stress field under thermal-load

In this study, we mainly focus on the intensity of singular stress field ISSF at the end of coating layer under the thermal shock test. The optimization will be done from the results of ISSF affected by the coating thickness. In the previous studies, a convenient method for the solution of ISSF in an adhesive bonding plate under bending and tension has been proposed. [8, 9] And in this paper, the method is applied to analysis the coating problem under thermal shock.

For bonded structure shown in **Figure 1 (f)**, in JIS test and our former research, it is known that the most dangerous point is at the end of the interface, where the stress goes infinity with its singularity of $\sigma_{ij} \propto 1/R^{\lambda}$, in which R is the distance from the end of the interface in a dissimilar bonded structure(see **Fig 5(b)**). Here λ is singular index, which is the root of **Equation 1**. [10, 11] As for α and β in **Equation 1** are known as Dundurs' parameters which are expressed by **Equation 2**, [10, 11] where v is Poisson's ratio and $G = E/2(1+v)$ is shear modulus.

$$\left[sin^2\left(\frac{\pi}{2}\lambda\right) - \lambda^2 \right]\beta^2 + 2\lambda^2 \left[sin^2\left(\frac{\pi}{2}\lambda\right) - \lambda^2 \right]\alpha\beta + \lambda^2\left(\lambda^2 - 1\right)\alpha^2 + \frac{sin^2\left(\pi\lambda\right)}{4} = 0 \qquad (1)$$

$$\alpha = \frac{G_1\left(\kappa_2+1\right)-G_2\left(\kappa_1+1\right)}{G_1\left(\kappa_2+1\right)+G_2\left(\kappa_1+1\right)},$$

$$\beta = \frac{G_1\left(\kappa_2-1\right)-G_2\left(\kappa_1-1\right)}{G_1\left(\kappa_2+1\right)+G_2\left(\kappa_1+1\right)},$$

$$\kappa_j = \begin{cases} \dfrac{3-\nu_j}{1+\nu_j}\left(\text{plane stress}\right) \\ 3-4\nu_j\left(\text{plane strain}\right) \end{cases} \quad \left(j=1,2\right) \tag{2}$$

Since all properties of the three materials vary with temperature, the singular stress field is therefore changed by varying the material properties. The relationship between the singular index λ and the temperature is plotted in **Figure 4**. Singular index λ_2 for the interface between the bond coating and substrate is very close to 1, which means almost no singularity. Therefore, this study will mainly focus on the ISSF between the top coating and the bond coating as shown in **Figure 1(f)**. During the thermal shock test process as shown in **Figure 2(a)**, water-cooled condition is simulated by given temperature 20 ℃ to the entire surface of specimen at t=4800s, then the temperature distribution and thermal stress was determined by thermal and elastic analysis.

Thermal stress σ_r is caused by entire body temperature difference T + ΔT in the bonded structure shown in **Figure 5(a).** In our previous research for bonded pipe [12] and bonded cylinder [13], it is found that there is non-singular terms $\tilde{\sigma}_r$ in the stress component as shown in **Equation 3,** [13] which will cause difficulty in the solution of ISSF. Therefore it is necessary to eliminate the non-singular term. There is also another non-singular term σ_0 caused by thermal stress[14]. By eliminating the non-singular terms σ_0, and $\tilde{\sigma}_r$, the remaining singular term $(\sigma_y - \sigma_0 - \tilde{\sigma}_r)$ has a singularity of the form $r^{1-\lambda}$as shown in **Equation 4**.

$$\sigma_r^{Axial} - \sigma_0 = \lim_{r\to 0}\frac{K_\sigma^{Axial}}{r^{1-\lambda}} + \tilde{\sigma}_r = \lim_{r\to 0}\frac{K_\sigma^{Axial}}{r^{1-\lambda}} + -\frac{\left(\nu_1-\nu_2\right)E_1E_2}{\left(1+\nu_1\right)\nu_1 E_2 - \left(1+\nu_2\right)\nu_2 E_1}\frac{u_{r0}^{AXIAL}}{\left(W+R_{inf}\right)} \tag{3}$$

$$\sigma_r^{Axial} - \sigma_0 - \tilde{\sigma}_r = \lim_{R\to 0}\frac{K_\sigma^{Axial}}{R^{1-\lambda}} \tag{4}$$

This intensity of singular stress field caused by thermal stress is equivalent to the one due to the remote tension σ_0 as shown in **Equation 5**. [8]

$$\sigma_0 = -\Delta\alpha\Delta E\Delta T, \tag{5}$$

where,

$$\Delta\alpha = \begin{cases} \alpha_1 - \alpha_2 & (\text{plane stress}) \\ (1+\nu_1)\alpha_1 - (1+\nu_2)\alpha_2 & (\text{plane strain}) \end{cases}$$

$$\Delta E = \frac{8}{\left\{ \dfrac{(\kappa_1 - 3)}{G_1} - \dfrac{(\kappa_2 - 3)}{G_2} \right\}}$$

$$\kappa_j = \begin{cases} \dfrac{3-\nu_j}{1+\nu_j} & (\text{plane stress}) \\ 3 - 4\nu_j & (\text{plane strain}) \end{cases}$$

$$G_i = \frac{E_i}{2(1+\nu_i)} \begin{pmatrix} i = 1 : \text{Top coat,} \\ i = 2 : \text{Middle coat} \end{pmatrix}$$

The problem of finite bonded plate subjected to tension shown in **Figure 5(b)** has been accurately calculated by using the body force method [15, 16]. Since the singular stress fields are similar if the material angles of two bonded structures are the same, then the stress intensity of unknown problem shown in **Figure 5(a)** can be determined by applying this known solution (**Figure 5(b)**) to **Equation 6**. [8-9, 17]

$$\frac{K_\sigma}{K_\sigma^*} = \frac{F_\sigma \sigma_0 W^{1-\lambda}}{F_\sigma \sigma_0^* W^{1-\lambda}} = \frac{\sigma_{r,FEM} - \sigma_0 - \tilde{\sigma}_r}{\sigma_y^{FEM*}} \tag{6}$$

Here the superscript * means known reference problem.

To verify application of proportional method expressed as **Equation 6**, a basic bonded axi-symmetric problem is investigated under thermal load. Considering the thickness of coating is usually small enough compared to the inner radius of the roll, the inner radius of the basic model is assumed as infinite (**Figure 6(a)**). Here we use $W/R_{inf}=10^{-5}$. **Table 2** shows the FEM results of stress for these two problems with using different minimum

8

element size of $2.25×10^{-7}$mm and $2.25×10^{-8}$ mm respectively. The thermoelastic constant term σ_0 and the non-singular term $\tilde{\sigma}_r$ are also listed in the table. The value $\sigma_{r0,FEM}^{Axial}$ and $\sigma_{y0,FEM}^{*}$ in **Table 2** are FEM solutions which are usually mesh dependence. However, the stress ratio $(\sigma_{r0,FEM}^{Axial} - \sigma_0 - \tilde{\sigma}_r)/\sigma_{y0,FEM}^{*}$ is independent of mesh size when same material property and FE mesh pattern are applied to the two problems. This means the FEM error can be eliminated by applying the same mesh pattern and the same minimum element size to the unknown problem and reference problem. This also reveals that the elimination of the non-singular terms in the stress of axi-symmetric problems under thermal load is correct. In view of the fact that the exact solution of the reference problem shown in **Figure 6(b)** has already been obtained [15,17], the ISSF for the unknown axi-symmetric problem can be solved by applying **Equation 6**.

5. **Results and Discussion for the Intensity of Singular Stress Field**

The model dimensions used in the analysis are shown in **Figure 7** with the local FEM mesh near the end of interface between top coating and bond coating. The minimum element size near the end of interface is e_{min}=$2.3438×10^{-5}$mm. The total number of the element is 5120.

 Figure 8 shows the stress history at the end of interface around the water cooling. In FEM simulation the largest singular stress appears just after dipping into the water, however K_σ takes a maximum value at the steady state under constant temperature of 1000℃ and decreases immediately after the start of cooling. This behavior was confirmed in our previous study. [6] Therefore in this research we mainly pay attention to the condition of temperature 1000 ℃. It is also found that the top material 8YZ, which means the content of Y_2O_3 is 8%, has the best thermal shock resistance among the three

materials. This result coincides with the experimental result shown in **Figure 2(b)**. Therefore the following research will mainly focus on the structure with top coating of 8YZ.

To investigate the effect of the coating thickness on the intensity of singular stress field, the top coating thickness H and the bond coating thickness h of the FEM model were changed systematically. As shown in **Figure 7(a)**, the thickness of top coating **H** was changed from 0.05mm to 0.30mm while the thickness of bond coating **h** was changed from 0.025mm to 0.15mm. And the results of K_σ are listed in **Table 3(a)**.

From **Table 3(a)** it is found that the model with thinner top coating thickness always has smaller K_σ. In other words, the thinner top coating has better thermal shock resistance. The results for each H constant in **Table 3(a)** were plotted in **Figure 9**. It is found that the singular stress intensity reaches the minimum value when the coating thickness ratio of top coating and the bond coating H/h≅2, which is in accordance with the results for plane strain state model shown in **Table 3(b)** [6]. This also coincides with the conventional knowledge of spray coating companies.

It is important to understand the difference between the model specified by JIS8304 and the actual axi-symmetric model to evaluate the debonding strength of the ceramic spray coating accurately. From this view point the ratios of $K_\sigma^{plane}/K_\sigma^{axial-symmetric}$ are shown in **Table 3(c)**. For different coating thickness, the ISSF of these two problems change in a similar way, which means the optimum conditions are also similar. In **Table 3(c)** all ratios are larger than 1, which means the ISSF of axi-symmetric strain problem is always smaller than that of plane strain problem. The results in **Table 3(c)** indicate that the ISSF of plane strain in the JIS specimen model is approximately 20% larger than the same place of the real shaped cylindrical model. Since the JIS standard is relatively more severe, it can be used to evaluate the roll coating strength safely.

6. **Conclusions**

This paper focuses on the intensity of singular stress field (ISSF) appearing at the end of ceramic spray coating layers of hearth roll under thermal loading by varying the coating thickness and top coating material. The conclusions can be summarized in the following way.

(1) The difference between the roll cylindrical shape and the plane strain JIS specimen was clarified. It is found that ISSF of JIS specimen is larger than the ISSF of cylindrical shape by 20%. Therefore, by using JIS specimen the coating strength can be evaluated safely.

(2) Under constant top coating thickness, the ISSF reaches the minimum value when the coating thickness ratio of the top coating and the bond coating H/h≅2, which is in accordance with the previous research assuming plane strain of JIS specimen.

(3) The top coating material 8YZ having the minimum content of Y_2O_3 shows the best performance of thermal shock resistance because of small value of ISSF.

(4) The analysis method of ISSF for axi-symmetric cylindrical layers was considered by applying FEM under thermal loading. It was found that by eliminating the non-singular term $\tilde{\sigma}_r$ and thermal constant σ_0 from the FEM stress ISSF can be obtained accurately by using mesh independent technique.

11

[1]   W. Lankford, N. Samways, R. Craven, and H. McGannon, *The Making, Shaping and Treating of Steel*, Association of Iron and Steel Engineers, Pittsburgh, PA USA **1985.**

[2]   S. Kasai, Y. Sato, A. Yanagisawa, A. Ichihara, and H. Onishi, *Kawasaki Steel Technical Report.* **1987**, *17*, 81.

[3]   M. Sawa and J. Oohori, presented at the 14th International Thermal Spray Conf., Kobe, Japan, May, **1995.**

J. W. Choi and D. Kim, ISIJ Int. **1999**, *39* 823.

[4]   JIS H 8304, Ceramic Thermal Spraying, Japanese Industrial Standards Committee, **2007**.

[5]   Y. Mutoh, I. Sakamoto, O. Waranabe and T. Nishimura, *Quarterly Journal of the Japan Welding Society*. **1989**, *7*, 208.

[6]   N. A. Noda, T. Uchikoba, M. Ueno, Y. Sano, K. IIda, Z. Wang and G. Wang, *ISIJ, Int.*, **2015**, *55*, 2624.

[7]   R.L. Hao, presented at ASM International Conf. Beijing, China, May, **2007.**

[8]   Y. Zhang, N. A. Noda, P. Wu and M. Duan, *International Journal of Adhesion and Adhesives*, **2015**, *57*, 105. ; Y. Zhang, N. A. Noda, P. Wu and M. Duan, *International Journal of Adhesion and Adhesives*, 2015, 60, 130.

[9]   N. A. Noda, T. Miyazaki, R. Li, T. Uchikoba, Y. Sano and Y. Takase, *International Journal of Adhesion and Adhesives*, **2015**, *61*, 46.

[10]   D. B. Bogy, *Trans. of the ASME. Jour. Appl. Mech.*, **1971**, *38*, 377.

[11]   D. B. Bogy, *Trans. of the ASME. Jour. Appl. Mech.*, **1968**, *35*, 460.

[12]   N. A. Noda, Z. Wang, K. Iida, Y. SANO and T. Miyazaki, *Journal of the Society of Materials Science Japan*, **2016**, *65*, 443.

[13]   T. Miyazaki, N. A. Noda, Z. Wang, and Y. SANO, *Trans. JSME*, **2015**, *81*, 1.

[14]   S. Ioka, S. Kubo, K. Ohji and J. Kishimoto, *Trans. Jpn. Soc. Mech. Eng. A*, **1994**, *60*, 141.

[15]   D. H. Chen, and H. Nisitani, *Trans. Jpn. Soc. Mech. Eng. A*, **1993**, *59*, 2682.

[16]   N. A. Noda, R. Shirao, J. Li and J. S. Sugimoto, *Int. Journal of Solids and Structures*, **2007**, *44*, 4472.

[17]   T. Teranishi and H. Nishitani, *Trans. Jpn. Soc. Mech. Eng. A*, **1999**, *65*, 16.
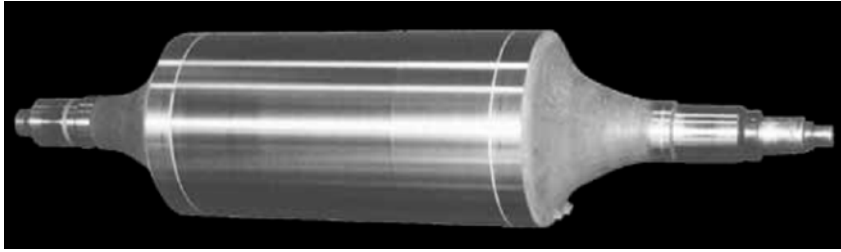
(a) Hearth roll used in continuous annealing line (CAL)
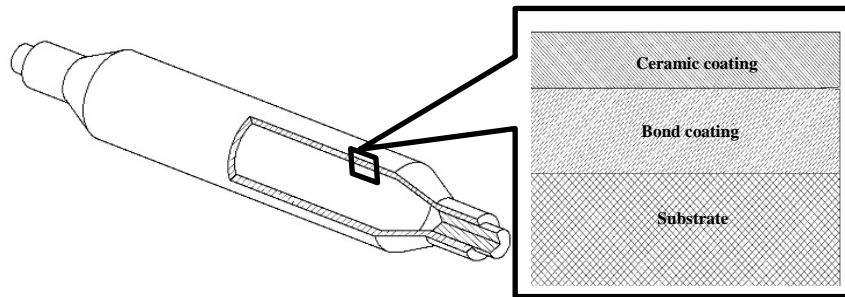
(b) Structure of hearth roll with spray
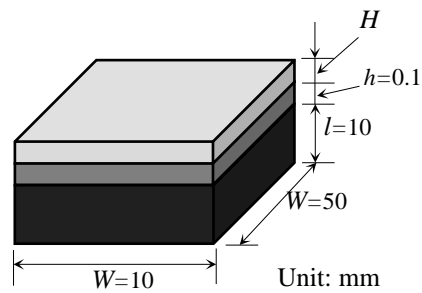
(c) JIS 8304 specimen for thermal shock test (plane strain)
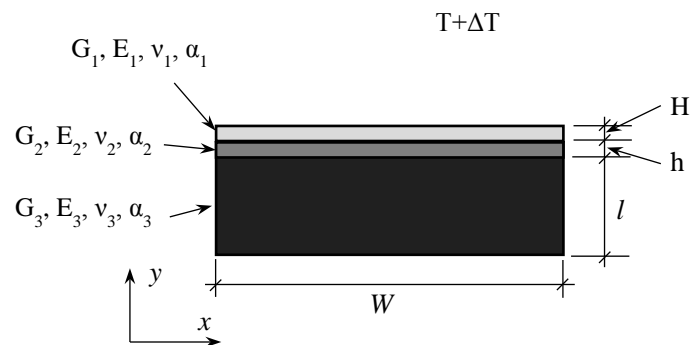
(d) Plane strain model of JIS specimen (xy-plane)

14
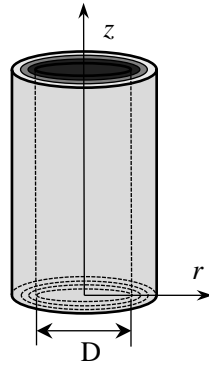
(e) Cylindrical structure of hearth roll (axi-symmetric)
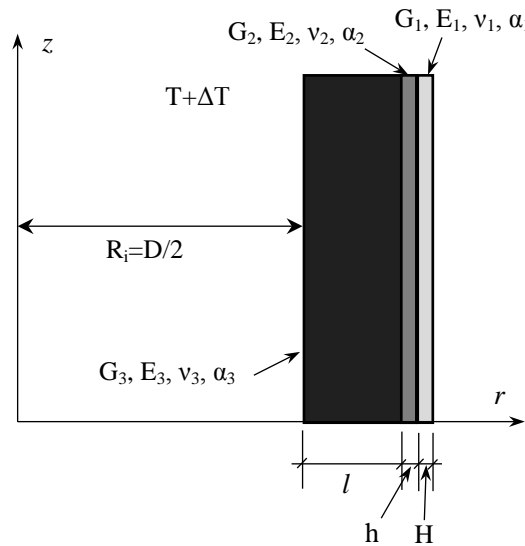
(f) Analysis model of axi-symmetric structure (rz-plane)

Figure 1. Analytical model of specimen in JIS and hearth roll used in CAL
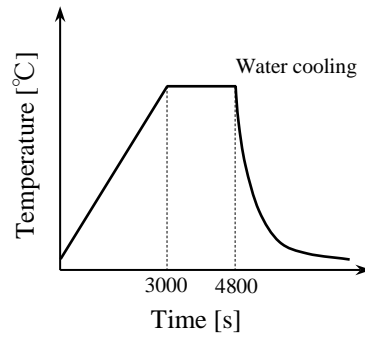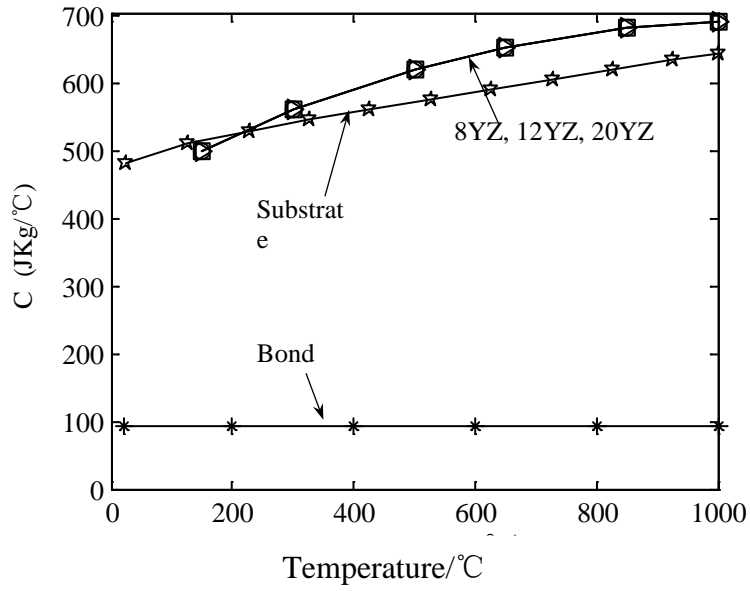
(a) Temperature history of thermal shock test in one cycle
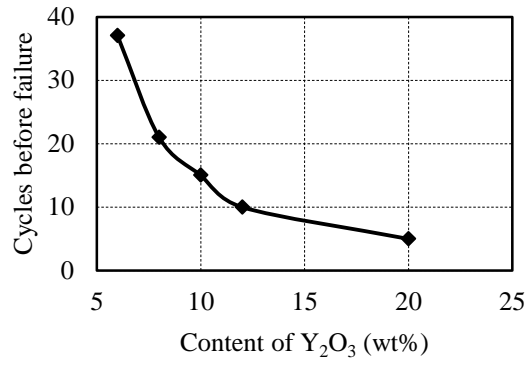
(b) Results of thermal shock test

Figure 2. Thermal shock test specified by JIS8304(2007)

(a) Coefficient of expansion

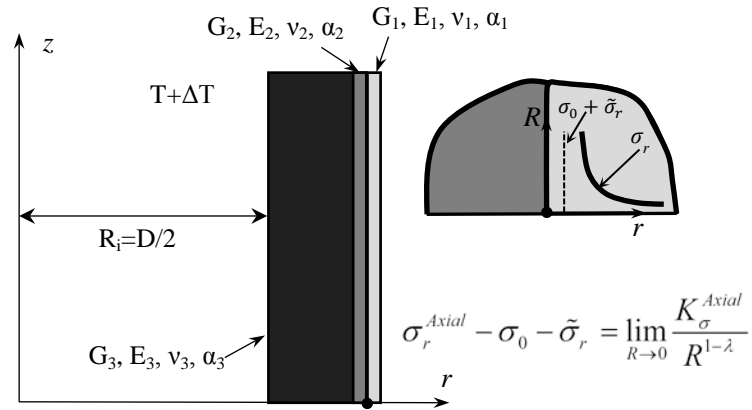(b) Specific heat

17
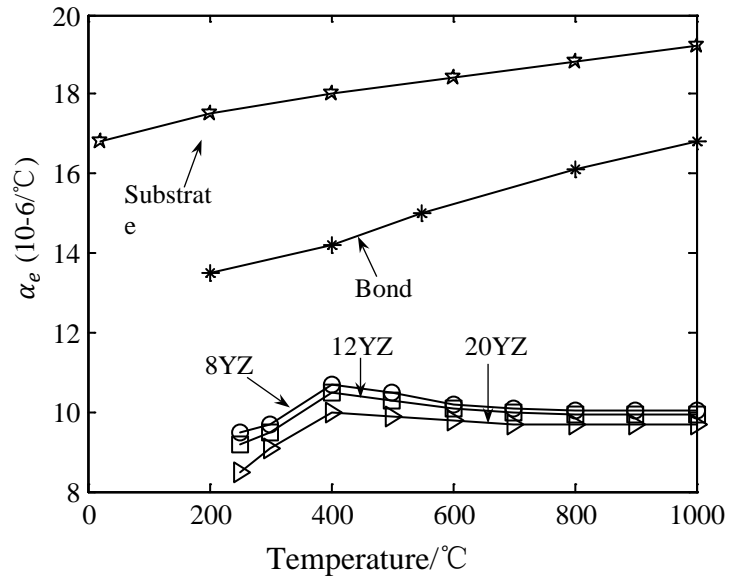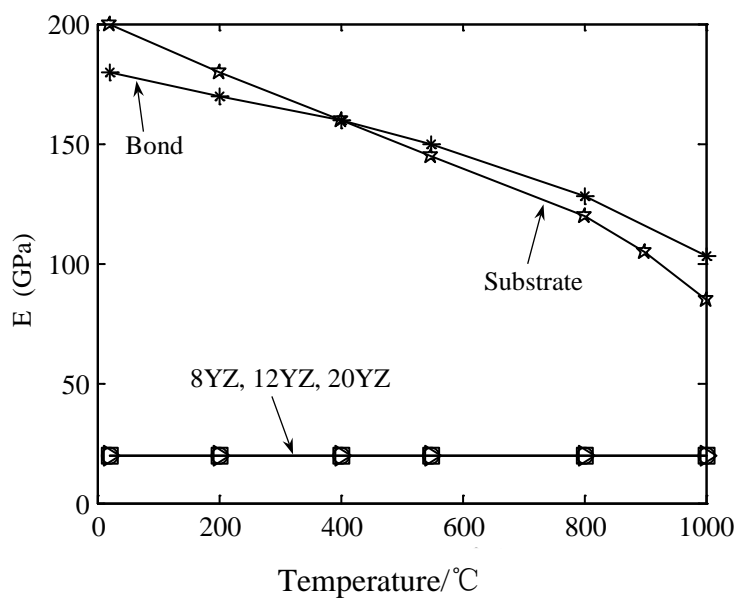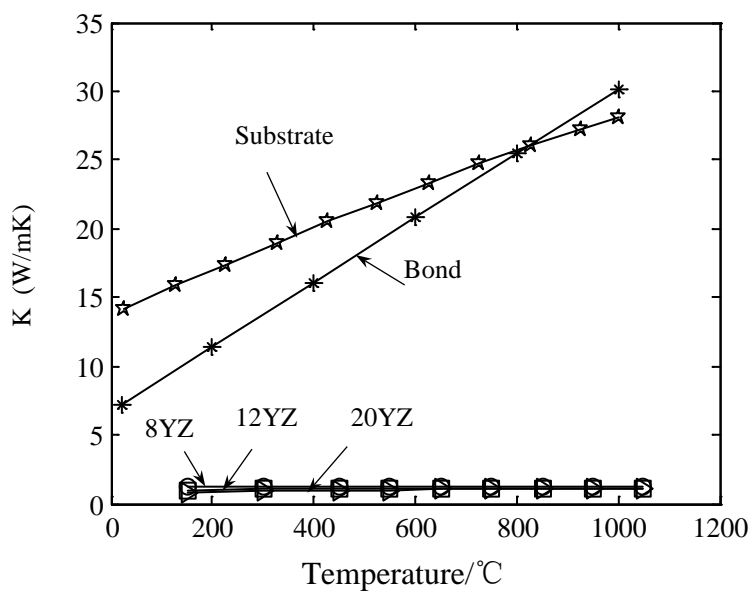
(c) Young's modulus

(d) Thermal conductivity

Figure 3. Relationship between material properties and temperature: a) coefficient of expansion; b) Specific heat; c) Young's modulus and d) Thermal conductivity
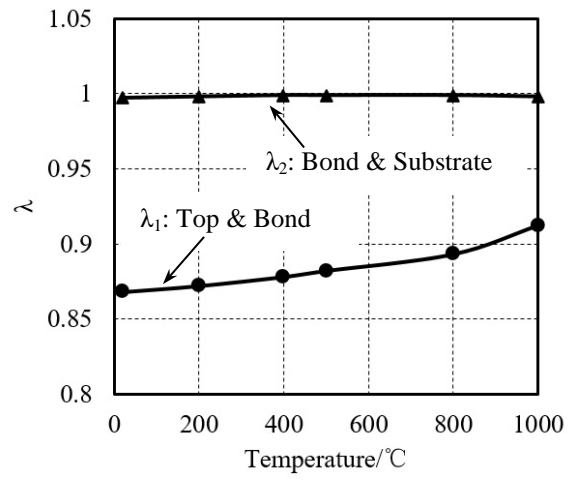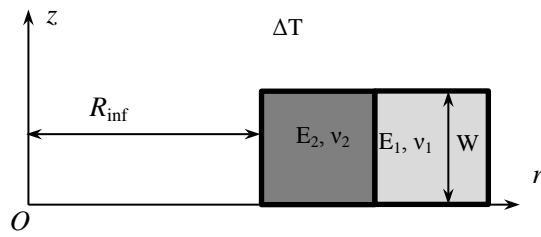
Figure 4. Relationship between temperature and singular index λ
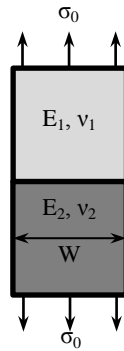
$$\sigma_r^{Axial} - \sigma_0 - \tilde{\sigma}_r = \lim_{R \to 0} \frac{K_\sigma^{Axial}}{R^{1-\lambda}}$$

(a) Thermal singular stress field for ceramic coating as unknown problem

$$\sigma_y^* = \lim_{R \to 0} \frac{K_\sigma^*}{R^{1-\lambda}}$$
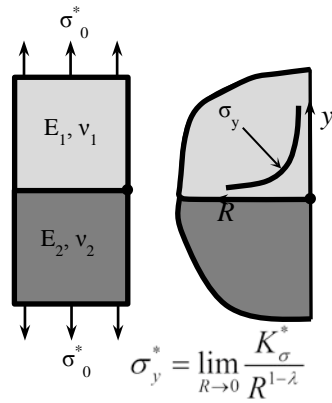
(b) The bonded strip model as the known reference problem

Figure 5. Comparison of reference problem and unknown problem
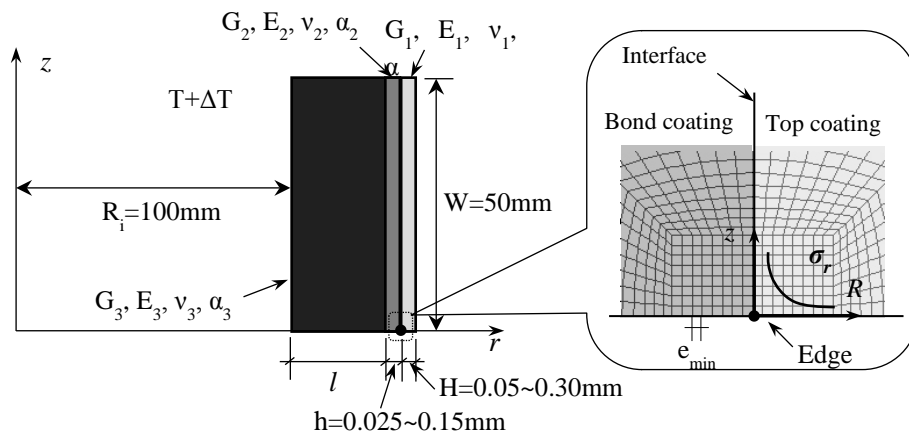
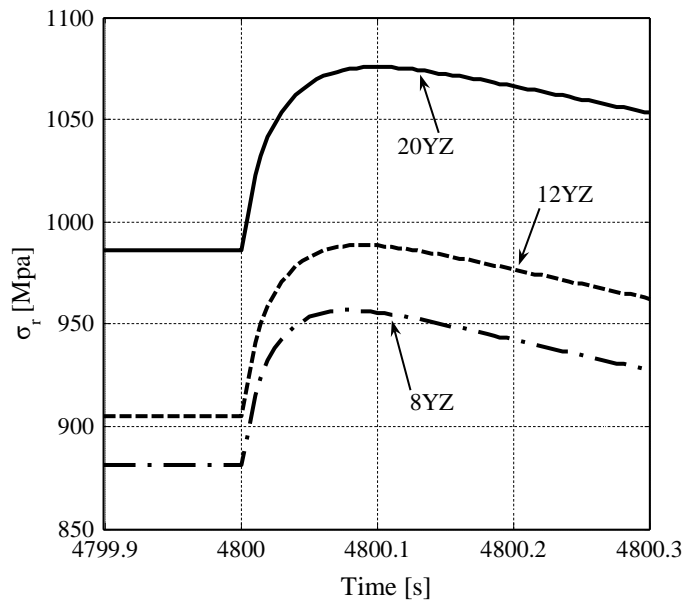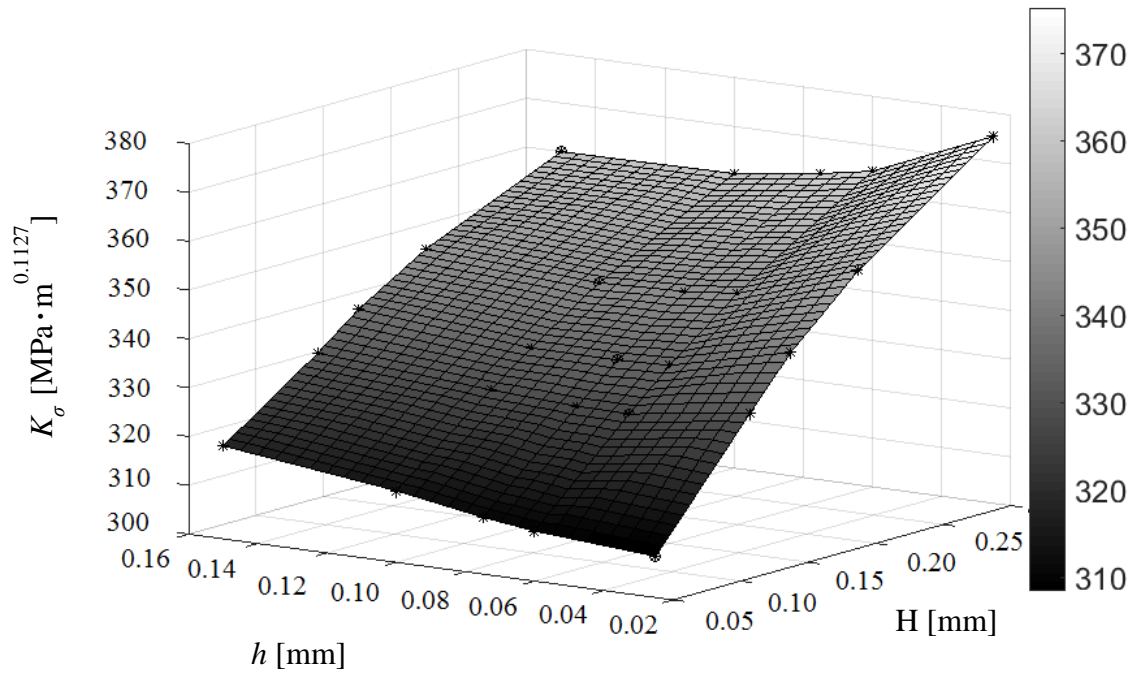(a) Basic axi-symmetric model

(b) Bonded plate

Figure 6. Basic axi-symmetric problem and bonded plate

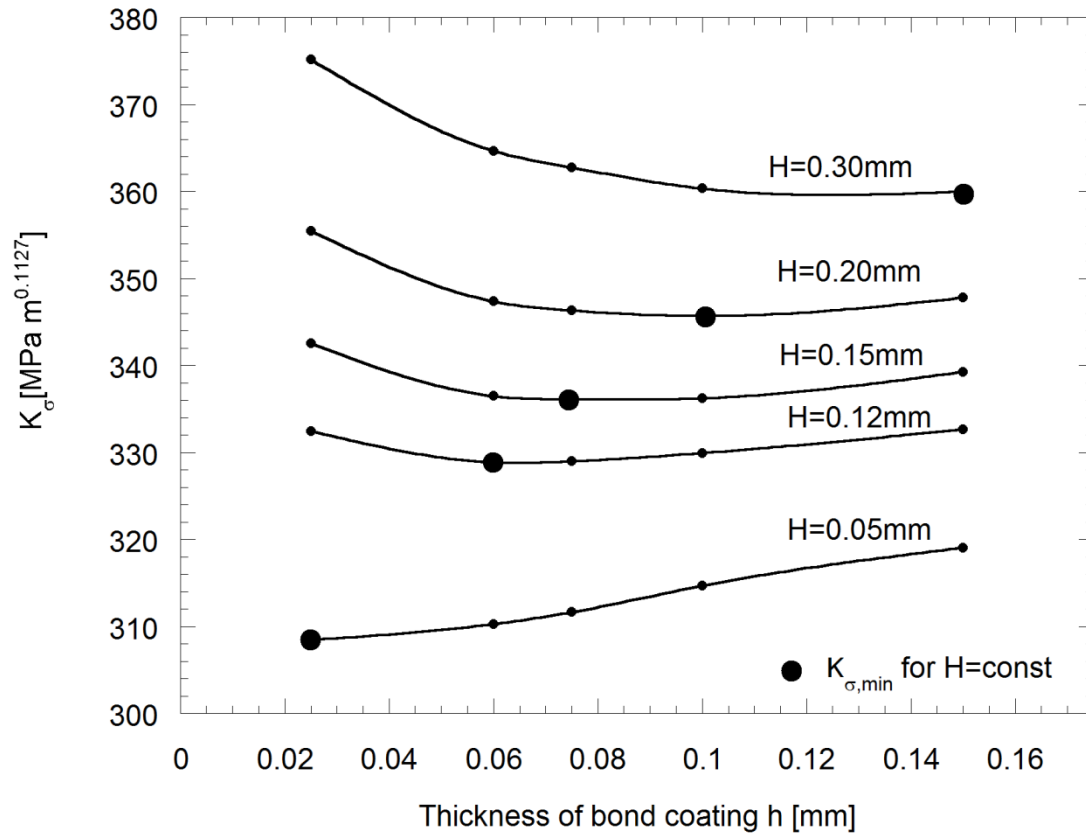**Figure 7.** Dimension of analysis model and local FEM mesh

Figure 8. Stress history at the end of interface around the water cooling

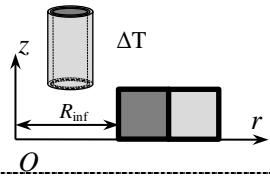(a) ISSF of different thickness of top coating (H) and bonded coating (h)
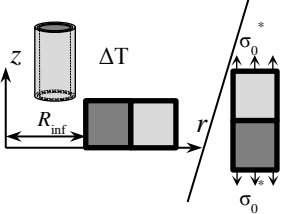
(b) ISSF of different thickness of of top coating (H) and bonded coating (h)

Figure 9. K_σ for 8YZ at 1000℃(axi-symmetric model)

Table 1. Material Properties depending on temperature

Material		Young's modulus E [GPa]	Poisson's ratio v	Thermal expansion $\alpha_e[10^{-6}/K]$
Top Coating	20YZ (ZrO_2-20wt%Y_2O_3)			7.5-9.7
	12YZ (ZrO_2-12wt%Y_2O_3)	20	0.25	8.3-9.93
	8YZ (ZrO_2-8wt%Y_2O_3)			8.7-10.05
Bonded Coating(CoNiCrAlY)		103-180	0.33	2.8-16.8
Substrate(SUS304)		85-200	0.3	16.8-19.2

Table 2 Stress components of bonded axi-symmetric problem and reference problem

Items	Stress components	$e_{min}/W=2.25\times10^{-7}$		$e_{min}/W=2.25\times10^{-8}$	
		Mat. 1	Mat. 2	Mat. 1	Mat. 2
	$\sigma_{r0,FEM}^{Axial}$	1.2689×10^{9}	1.6841×10^{9}	1.8654×10^{9}	2.4035×10^{9}
	$\tilde{\sigma}_{r0,FEM}^{Axial}$	9.8708×10^{7}	9.8708×10^{7}	9.8708×10^{7}	9.8708×10^{7}
	σ_{0}	-8.4354×10^{8}	-8.4354×10^{8}	-8.4354×10^{8}	-8.4354×10^{8}
	$\sigma_{y0,FEM}^{*}$	2.2750×10^{9}	2.7441×10^{9}	2.9489×10^{9}	3.5568×10^{9}
	$\sigma_{r0,FEM}^{Axial}\big/\sigma_{y0,FEM}^{Plate}$	0.55776	0.61372	0.63257	0.67575
	$\dfrac{\sigma_{r0,FEM}^{Axial}-\sigma_{0}-\tilde{\sigma}_{r0,FEM}^{Axial}}{\sigma_{y,FEM}^{*}}$	**0.8851**58	**0.8851**48	**0.8851**55	**0.8851**59

Table 3 (a). K_σ for 8YZ at 1000℃(axi-symmetric model)

Bond coating thickhess	H=0.05 mm	H=0.12 mm	H=0.15 mm	H=0.20 mm	H=0.30 mm
h=0.025mm	**308.44***	332.45	342.51	355.46	375.17
h=0.060mm	310.27	**328.85**	336.48	347.37	364.67
h=0.075mm	311.64	328.97	**336.09**	346.31	362.74
h=0.100mm	314.67	329.92	336.21	**345.67**	360.33
h=0.150mm	319.05	332.65	339.26	347.78	**359.98**

*(The figures in bold type show minimum value when H=const.) [MPa・m$^{0.1127}$]

Table 3 (b). K_σ for 8YZ at 1000℃ (plane strain model)[6]

Bond coating thickhess	H=0.05 mm	H=0.12 mm	H=0.15 mm	H=0.20 mm	H=0.30 mm
h=0.025mm	**366.27**[*]	407.27	419.34	435.87	460.77
h=0.060mm	370.48	**403.72**	413.93	428.68	451.35
h=0.075mm	371.24	404.05	**413.88**	427.83	449.68
h=0.100mm	373.59	405.05	414.31	**427.40**	448.05
h=0.150mm	376.81	407.73	416.30	428.27	**447.17**

*(The figures in bold type show minimum value when H=const.) [MPa$\cdot$m$^{0.1127}$]

Table 3 (c). $K_\sigma^{plane}/K_\sigma^{axial-symetric}$ for 8YZ at 1000℃

Bond coating thickhess	H=0.05 mm	H=0.12 mm	H=0.15 mm	H=0.20 mm	H=0.30 mm
h=0.025mm	1.1875	1.2251	1.2243	1.2262	1.2282
h=0.060mm	1.1941	1.2277	1.2302	1.2341	1.2377
h=0.075mm	1.1912	1.2282	1.2315	1.2354	1.2397
h=0.100mm	1.1872	1.2277	1.2323	1.2364	1.2435
h=0.150mm	1.1810	1.2257	1.2271	1.2316	1.2422